

Akt3 induces oxidative stress and DNA damage by activating the NADPH oxidase via phosphorylation of p47^{phox}

Christos Polytaichou^{a,b,c,d,1,2}, Maria Hatzia Apostolou^{b,c,d,1}, Tung On Yau^{b,c}, Niki Christodoulou^{b,c}, Philip W. Hinds^{d,e}, Filippos Kottakis^d, Ioannis Sanidas^{d,f}, and Philip N. Tsichlis^{a,d,2}

^aDepartment of Cancer Biology and Genetics, The Ohio State University Comprehensive Cancer Center, The Ohio State University, Columbus, OH 43210; ^bDepartment of Biosciences, John van Geest Cancer Research Centre, School of Science and Technology, Nottingham Trent University, NG11 8NS Nottingham, United Kingdom; ^cCentre for Health, Aging and Understanding Disease, Nottingham Trent University, NG11 8NS Nottingham, United Kingdom; ^dMolecular Oncology Research Institute, Tufts Medical Center, Boston, MA 02111; ^eDepartment of Developmental, Molecular and Chemical Biology, Tufts Cancer Center, Tufts University School of Medicine, Boston, MA 02111; and ^fDepartment of Medicine, Massachusetts General Hospital Cancer Center and Harvard Medical School, Charlestown, MA 02129

Edited by Peter K. Vogt, Scripps Research Institute, La Jolla, CA, and approved September 25, 2020 (received for review September 18, 2020)

Akt activation up-regulates the intracellular levels of reactive oxygen species (ROS) by inhibiting ROS scavenging. Of the Akt isoforms, Akt3 has also been shown to up-regulate ROS by promoting mitochondrial biogenesis. Here, we employ a set of isogenic cell lines that express different Akt isoforms, to show that the most robust inducer of ROS is Akt3. As a result, Akt3-expressing cells activate the DNA damage response pathway, express high levels of p53 and its direct transcriptional target miR-34, and exhibit a proliferation defect, which is rescued by the antioxidant *N*-acetylcysteine. The importance of the DNA damage response in the inhibition of cell proliferation by Akt3 was confirmed by Akt3 overexpression in *p53*^{-/-} and *INK4a*^{-/-}/*Arf*^{-/-} mouse embryonic fibroblasts (MEFs), which failed to inhibit cell proliferation, despite the induction of high levels of ROS. The induction of ROS by Akt3 is due to the phosphorylation of the NADPH oxidase subunit p47^{phox}, which results in NADPH oxidase activation. Expression of Akt3 in *p47*^{phox}^{-/-} MEFs failed to induce ROS and to inhibit cell proliferation. Notably, the proliferation defect was rescued by wild-type p47^{phox}, but not by the phosphorylation site mutant of p47^{phox}. In agreement with these observations, Akt3 up-regulates p53 in human cancer cell lines, and the expression of Akt3 positively correlates with the levels of p53 in a variety of human tumors. More important, Akt3 alterations correlate with a higher frequency of mutation of p53, suggesting that tumor cells may adapt to high levels of Akt3, by inactivating the DNA damage response.

Akt isoforms | NADPH oxidase | oxidative stress | DNA damage | cancer

The utilization of oxygen by all aerobic organisms gives rise to a heterogeneous group of molecules and radicals with distinct chemical properties, levels of reactivity, and biological impact, which are collectively known as reactive oxygen species (ROS). Under this term we include oxygen anions and radicals [superoxide (O⁻²) and hydroxyl radical (OH·)], singlet oxygen (¹O₂), hydrogen peroxide (H₂O₂), nitric oxide (NO·), peroxynitrite anions (ONOO⁻), and various peroxides (ROOR') and hydroperoxides (ROOH) (1, 2). Reactive oxygen species are generated by multiple mechanisms. Prominent among them are: 1) The escape of electrons during oxidative phosphorylation in the mitochondria. At least 2% of the electrons traveling along the respiratory chain in mitochondria escape and target oxygen to form superoxide (3, 4). 2) The enzymatic activation of the NOX family of NADPH oxidases. The multisubunit enzyme NADPH oxidase is most abundant in leukocytes, where it becomes activated when the cells engulf invading microorganisms. The activation of this enzyme promotes the rapid generation of superoxide whose sharp increase in these cells is known as the “respiratory burst” (5–7). Enzymes related to the leukocyte-specific NADPH oxidase are also present in other cell types (8). The preceding mechanisms produce ROS via processes endogenous to the cell (SI Appendix, Fig. S1). In addition to

the endogenous sources of ROS, there are exogenous sources such as environmental pollutants (4, 9).

NOX2, the first characterized NOX isoform, is an enzyme complex that mediates the transfer of electrons to molecular oxygen through the action of flavocytochrome b558, which is composed of two proteins gp91^{phox} and p22^{phox} and is located at the plasma membrane. Activation of the enzyme is induced via its association with a trimeric cytosolic protein complex, composed of p40^{phox}, p47^{phox}, and p67^{phox}. Upon stimulation by external signals, p47^{phox} undergoes phosphorylation and the trimeric complex translocates to the membrane to form the active oxidase by binding to b558 (10). The activation of the complex also requires two guanine nucleotide-binding proteins, cytosolic Rac2 and membrane-bound Rap1A (5, 11, 12). There are seven isoforms of gp91^{phox}, the catalytic transmembrane subunit of NOX. Based on this, the NOX family of oxidases consists of seven members, with each member exhibiting a distinct tissue distribution.

Signals originating in membrane receptors have been shown to induce ROS in a variety of cell types (13–15). ROS produced in

Significance

Although the three Akt isoforms share mechanisms of activation and exhibit overlaps in their downstream signaling pathways, significant differences are now being uncovered. Here, we show that among Akt isoforms, Akt3 preferably phosphorylates p47^{phox} and activates NADPH oxidase, resulting in robust induction of reactive oxygen species (ROS). Akt3-induced ROS activate the DNA damage response and upregulate p53 expression. Consequently, the proliferation rate of Akt3-expressing cells is reduced, an effect reversed by p53 loss. In cancer, Akt3 expression correlates with the abundance of p53; however, tumors can adapt to high Akt3 activity by inactivating the DNA damage response. These findings reveal differences in the regulation of ROS by Akt isoforms, which may be exploited therapeutically for Akt3-driven cancers.

Author contributions: C.P. and P.N.T. designed research; C.P., M.H., T.O.Y., N.C., F.K., and I.S. performed research; P.W.H. and P.N.T. contributed new reagents/analytic tools; C.P., M.H., and I.S. analyzed data; and C.P., M.H., and P.N.T. wrote the paper.

The authors declare no competing interest.

This article is a PNAS Direct Submission.

Published under the PNAS license.

¹C.P. and M.H. contributed equally to this work.

²To whom correspondence may be addressed. Email: christos.polytaichou@ntu.ac.uk or Philip.Tsichlis@osumc.edu.

This article contains supporting information online at <https://www.pnas.org/lookup/suppl/doi:10.1073/pnas.2017830117/-DCSupplemental>.

response to such signals function as second messengers by inducing reversible oxidation of a number of signaling molecules, including peroxiredoxins (16, 17) and various phosphatases, such as PTP-1B, SHP-2, and the tumor suppressor PTEN (18–20). Most relevant as a second messenger among ROS is H₂O₂, which is relatively stable and diffuses easily across biological membranes (21, 22). A critical target of ROS-producing signals originating in membrane receptors is the NADPH oxidase. Thus, ROS-producing insulin signals in adipocytes depend on NOX-4, a homolog of gp91^{Phox}, the catalytic subunit of NADPH oxidase (23). Although the function of some ROS may be physiologically important, persistence of ROS is generally harmful (3, 21). Their toxicity is due to irreversible oxidation of a variety of macromolecules such as DNA, lipids, carbohydrates, and proteins. To prevent ROS toxicity, cells employ a variety of detoxification mechanisms, which collectively are responsible for the very short half-life of ROS. The main mechanisms of ROS detoxification include: 1) ROS-induced oxidation of small antioxidant molecules; and 2) enzymatic conversion of ROS to less reactive species. Examples include the conversion of superoxide to H₂O₂ by superoxide dismutase, the conversion of H₂O₂ to H₂O and oxygen by catalase, and the action of peroxiredoxins. The overall levels of ROS in cells are determined by the balance between the rate of production and the rate of conversion (3, 17, 24, 25).

Akt1, also known as protein kinase B α (PKB α), is the founding member of a protein kinase family composed of three members, Akt1, Akt2, and Akt3. Akt family members regulate a diverse array of cellular functions and play important roles in most types of human cancer. Akt activation depends on PtdIns-3,4,5-P₃, and to a lesser extent on PtdIns-3,4-P₂, both of which are products of phosphoinositide 3-kinase (26, 27). The interaction of PtdIns-3,4,5-P₃ with the PH domain of Akt, promotes the translocation of Akt to the plasma membrane where it undergoes phosphorylation at two sites, one in the activation loop and one in the carboxyl-terminal tail (26–28). Phosphorylated Akt may translocate from the plasma membrane to the cytosol or the nucleus. Activated Akt ultimately undergoes dephosphorylation by phosphatases and returns to the inactive state (29).

Recently, we and others showed that despite their sequence similarity, Akt isoforms exhibit dramatic signaling differences (30–35). Data in this study show that although all Akt isoforms up-regulate the cellular levels of ROS, it is Akt3, which exhibits maximum activity. Akt2-expressing cells are also characterized by relatively high levels of superoxide. However, the levels of H₂O₂ in these cells are very low, perhaps because they express low levels of superoxide dismutase 1 and 2 (SOD1 and SOD2). Akt3 promotes the accumulation of superoxide and H₂O₂ by preferentially activating the NADPH oxidase through p47^{Phox}. The high levels of ROS in Akt3-expressing cells induce DNA damage. This activates the DNA damage response, which inhibits cell proliferation. The levels of Akt3 in several types of human cancer correlate with the levels of p53. More important, *Akt3* amplification correlates positively with the mutation of *p53*. Our data suggest that tumor cells may adapt to Akt3 expression by inactivating the DNA damage response pathways.

Experimental Procedures

Expression Constructs. Expression constructs of Myc-Akt1, Myc-Akt2, and Myc-Akt3 in the retroviral pBabe vectors were described earlier (30, 32, 33). Human p47^{Phox} was cloned in the vector pBabe-bleo. Ser and Thr to Ala mutations were introduced into this vector by the QuikChange II Site-Directed Mutagenesis Kit (Agilent, Inc.).

Cells and Culture Conditions. Akt1-, Akt2-, and Akt3-expressing and *Akt1/Akt2/Akt3* triple knockout (*TKO*) lung fibroblasts have been described previously (30, 32, 33). Briefly, lung fibroblasts cultured from an *Akt1^{fl/fl}/Akt2^{-/-}/Akt3^{-/-}* mouse were spontaneously immortalized via a 3T3-type protocol. The immortalized cells were transduced with retroviral constructs of Myc-Akt1, Myc-Akt2, or Myc-Akt3 in the retroviral vector pBabe-puro, neo, bleo,

or GFP. Subsequently, they were transduced with a MigR1-Cre-hygro construct to ablate the floxed *Akt1* allele. This gave rise to isogenic Akt1-, Akt2-, or Akt3-expressing cells. To generate the *TKO* cells, the *Akt1^{fl/fl}/Akt2^{-/-}/Akt3^{-/-}* lung fibroblasts were transduced with the MigR1-Cre-hygro construct and the transduced cells were selected with hygromycin. Cells were used soon after selection, because they do not proliferate but remain viable for about a week (33). The Akt1-, Akt2-, Akt3-, and Akt1/2/3-expressing cells and the *TKO* lung fibroblasts were cultured in DMEM (Dulbecco's Modified Eagle Medium) supplemented with 10% FBS (fetal bovine serum) and antibiotics. Selected cultures were treated with 5 mM of the antioxidant N-acetylcysteine (NAC, A7250, Sigma-Aldrich).

p47^{Phox}-/- mice were previously described (36). Mouse embryonic fibroblasts (MEFs) derived from these and wild-type C57BL/6 mice were cultured and spontaneously immortalized by serial passaging. The immortalized *p47^{Phox}-/-* MEFs were transduced with the wild-type or mutant *p47^{Phox}* constructs. *P53^{-/-}* (37) and *INK4a/Arf^{-/-}* (38) MEFs were previously described. Primary and spontaneously immortalized MEFs were cultured in DMEM supplemented with 10% FBS and antibiotics. The breast cancer cell lines MDA-MB-231, and T-47D (ATCC) were cultured in RPMI 1640 supplemented with 10% FBS and antibiotics. Melanoma cell lines SKMEL2, LoxMVII, and UACC62 were cultured in DMEM supplemented with 10% FBS and antibiotics.

Quantitative RT-PCR. qRT-PCR was used to measure the levels of expression of the microRNAs miR34a, miR34b, and miR34c and the SOD isoforms, SOD1, SOD2, and SOD3. For the measurement of the microRNA levels, we used miRCURY LNA Universal RT and LNA PCR primer sets for miR-34a, miR-34b, miR-34c (204486, 204005, and 204407 respectively, Exiqon). For the measurement of the SOD levels, we used the following primer pairs: CCAGCATGGGTCCACGTCCAT and CGCCGGGCCACCATGTTTCTT (SOD1), TCGCTACAGATTGCTGCCTGCT and AAGCGTGCTCCCACAGTCA (SOD2), and CTCTAGCTGGGTGCTGGCCTGA and CGCGCCAGTAGCAAGCCGTAG (SOD3). Gene expression levels were normalized against U6, and b-actin and GAPDH for microRNAs and SODs, respectively.

Intracellular Levels of ROS, Protein and Glutathione Oxidation, and Antioxidant Activity. Cells were treated with 5-(and-6)-carboxy-2',7'-dichlorofluorescein diacetate (carboxy-DCFDA) (10 μ M), dihydroethidium (DHE) (5 μ M), or Mitotracker Red CM-H2XRos (MitoROS) (Invitrogen) (2 μ M), in DMEM without phenol red. ROS-induced fluorescence in these cells was measured by flow cytometry. Global protein oxidation, reduced glutathione/glutathione disulfide (GSH/GSSG) ratios, and total cell antioxidant activity were measured with the OxyBlot Protein Oxidation Detection Kit (S7150), Glutathione Assay Kit (CS0260), and Antioxidant Assay Kit (CS0790, Sigma), respectively, according to the instructions of the manufacturer.

Single-Cell Gel Electrophoresis Assay. DNA damage was measured using the CometAssay (Trevigen), as previously described (39). Akt1- and Akt3-expressing lung fibroblasts were suspended in molten low-melting-point agarose and spread onto the CometSlide. Cells were lysed, and following alkaline gel electrophoresis, they were stained with SyBrGreen I. Fluorescent SyBrGreen I-bound DNA was photographed using a Nikon Eclipse 80i microscope with a 20 \times objective and a spot charge-coupled device camera (Diagnostic Instruments). To measure DNA damage, the comet tail intensity and length were quantified using Comet Assay IV software (Perceptive Instruments).

TUNEL Assay. Apoptosis was measured using a terminal deoxynucleotidyl-transferase biotin-dUTP nick end labeling (TUNEL) kit (Roche) (39).

Antibodies, Immunoprecipitation, and Western Blotting. Akt1-, Akt2-, and Akt3-specific antibodies, as well as antibodies against p53, flag-tag, phosphorylated Akt substrate (RXXS/T), and phosphorylated histone H2AX on Ser139, were purchased from Cell Signaling Technology. Cells were lysed using radioimmunoprecipitation assay (RIPA) cell lysis buffer (Cell Signaling Technology) supplemented with protease and phosphatase inhibitors (Roche). Immunoprecipitation (IP) assays were performed with mouse DYKDDDDK Tag (9A3) antibody and Protein G magnetic beads and Western blots of electrophoresed immunoprecipitates were probed with rabbit Phospho-Akt substrate and TrueBlot secondary antibodies (Rockland, Inc.). Western blots of electrophoresed cell lysates were probed with the indicated antibodies, following standard procedures.

Results

Triple *Akt* Knockout Lung Fibroblasts, Rescued by *Akt3*, Grow Slower than the *Akt1*- or *Akt2*-Rescued Cells. Lung fibroblasts and kidney-derived cells from *Akt1^{fl/fl}/Akt2^{-/-}/Akt3^{-/-}* mice were spontaneously immortalized, as previously described (32, 33). The immortalized cells were transduced with retroviral constructs of *Akt1*, *Akt2*, or *Akt3*, or with the empty retroviral vector. Knocking out the floxed *Akt1* allele in these cells with Cre, gave rise to otherwise identical cell lines that express one *Akt* isoform at a time, or they are *Akt*-null. The physiological relevance of exogenous *Akt* expression was confirmed by experiments comparing the rate of proliferation of *Akt1*-rescued cells with the rate of proliferation of *Akt1^{fl/fl}/Akt2^{-/-}/Akt3^{-/-}* and *Akt*-null cells. These experiments showed that cells expressing endogenous and exogenous *Akt1* exhibit similar rates of proliferation (*SI Appendix*, Fig. S2). Monitoring the expression of the three *Akt* isoforms in serially passaged cells by Western blotting revealed that although all *Akt* isoforms were expressed well in early passage cells, *Akt3* expression decreased progressively in subsequent passages (Fig. 1A). This observation suggested that cells expressing high *Akt3* levels may proliferate slower and may therefore be counterselected over time. To address this hypothesis, *Akt1*-, *Akt2*-, *Akt3*-, and *Akt1/2/3*-expressing cells were plated at equal densities and their proliferation rates were monitored by counting them daily for 3 d. The results confirmed that the proliferation of *Akt3*-expressing cells lagged behind the proliferation of cells expressing *Akt1*, *Akt2*, or *Akt1/2/3* (Fig. 1B). The slow proliferation of *Akt3*-rescued cells did not depend on the cell type, as it was also observed in *Akt3*-rescued kidney-derived cell lines (*SI Appendix*, Fig. S3).

***Akt3* Expression Activates the DNA Damage Response.** Our earlier studies showing that spontaneously immortalized lung fibroblasts from triple *Akt* knockout mice engineered to express *Akt1*, *Akt2*, or *Akt3*, exhibit dramatic differences in microRNA profiles (33), provided a potential explanation for the inhibitory effects of *Akt3* on cell proliferation and survival. One microRNA family that is induced upon IGF1 stimulation in *Akt3*-, and to a lesser extent in *Akt2*-expressing cells is the miR-34 family (Fig. 2A). The real time RT-PCR data in Fig. 2B confirmed the results of the microarray analysis. Given that the miR-34 microRNA family is a direct transcriptional target of p53 (40), we examined the expression of p53 in these cells. The results in Fig. 2C revealed that p53 is also up-regulated by *Akt3*.

Given that p53 and the miR-34 microRNAs inhibit cell proliferation (40–42), we hypothesized that the inhibitory effects of *Akt3* on cell proliferation may be mediated by p53 and its

transcriptional target, miR-34. The data in Fig. 2D and E show that high *Akt3* expression coincides with high levels of p53 and low cell proliferation rates and they support the hypothesis that p53 and miR-34 are the mediators of the *Akt3*-induced inhibition of cellular proliferation.

p53 is induced by DNA damage (43, 44). The high levels of p53, in *Akt3*-expressing cells, therefore, suggested that *Akt3* expression may promote DNA damage and the activation of the DNA damage response. To address this question, we examined the phosphorylation of histone variant H2A.X (γ -H2A.X) (45, 46) in passaged *Akt3*-rescued cells expressing progressively lower levels of *Akt3* and p53. The results showed that the phosphorylation of H2A.X, an established marker of DNA damage, decreases with each passage, in parallel with the *Akt3* and p53 (Fig. 2F). In agreement with this observation, DNA damage was more pronounced in *Akt3*-expressing cells, as determined by the Comet assay. The same cells were also characterized by a higher apoptotic index, as determined by the TUNEL assay (*SI Appendix*, Fig. S4). These data suggest that *Akt3* expression is indeed associated with DNA damage and with the activation of the DNA damage response.

***Akt* Isoforms Differentially Regulate the Generation of ROS.** Given that *Akt*-transduced signals have been linked to the up-regulation of the cellular levels of ROS (44, 47–51), we hypothesized that the DNA damage and the induction of p53 and miR-34 in *Akt3*-expressing cells may be caused by reactive oxygen species induced differentially by *Akt* isoforms. To address this hypothesis, the triple *Akt* knockout lung fibroblasts and their derivatives expressing *Akt1*, *Akt2*, or *Akt3*, were loaded with DCFDA or DHE and analyzed by flow cytometry. DCFDA fluoresces upon interaction with a variety of reactive oxygen species (primarily H₂O₂), while DHE exhibits significant specificity for superoxide (52). The results in Fig. 3A show that the highest levels of DCFDA-specific ROS (H₂O₂) were detected in *Akt3*-expressing cells and the lowest in *Akt2*-expressing cells. The *Akt1*-expressing cells harbored intermediate levels of H₂O₂. The results in Fig. 3B show that the highest levels of DHE-specific ROS (superoxide) were detected again in *Akt3*-expressing cells. *Akt2*-expressing cells, however, which harbored low levels of H₂O₂ (Fig. 3A), had increased superoxide levels, slightly lower than those detected in *Akt3*-expressing cells. The levels of superoxide in *Akt1*-expressing cells were low, relative to its levels in *Akt2*- and *Akt3*-expressing cells. Fig. 3C shows that platelet-derived growth factor (PDGF) and serum stimulation of serum-starved cells induce DCFDA-detectable ROS (H₂O₂). In agreement with data in Fig. 3A, H₂O₂ induction was again highest in *Akt3*- and lowest in *Akt2*-expressing cells.

The relationship of DCFDA- and DHE-detectable ROS (H₂O₂ and superoxide, respectively) in *Akt*-expressing cells may be due to differences in the level and activity of SOD, the enzyme that converts superoxide into H₂O₂. There are three isoforms of SOD: SOD1 or Cu/ZnSOD, which is localized in the nucleus and the cytoplasm; SOD2, or MnSOD, which is localized in the mitochondria; and SOD3, which is membrane bound (53). Based on the preceding data, we hypothesized that the expression of SODs may be lower in *Akt2*-rescued cells. Quantitative RT-PCR confirmed the prediction by showing that *Akt2*-rescued cells indeed express lower levels of the two main isoforms of this enzyme, SOD1 and SOD2 (Fig. 3D).

Reactive oxygen species modulate the cellular phenotype in part by oxidizing glutathione and cellular proteins. We therefore examined the GSH/GSSG ratio and the abundance of oxidized proteins in cellular extracts of triple *Akt* knockout lung fibroblasts and their derivatives expressing *Akt1*, *Akt2*, or *Akt3*. To determine the GSH/GSSG ratio, we measured the levels of reduced and oxidized glutathione in deproteinized extracts derived from equal numbers of these cells. The results showed that, following serum starvation for 6 h, the ratio was similar in all of the cell lines.

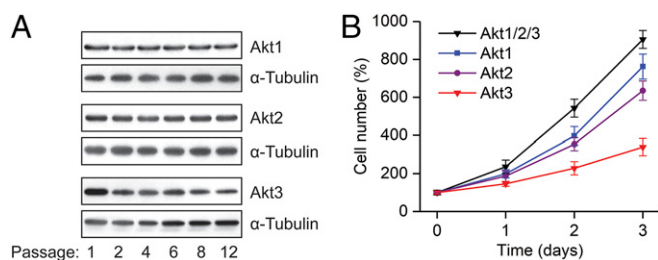


Fig. 1. Triple *Akt* knockout lung fibroblasts engineered to express *Akt3* proliferate more slowly than isogenic lung fibroblast lines expressing *Akt1* or *Akt2*. (A) Whereas the expression of *Akt1* and *Akt2* remains stable, *Akt3* expression declines with cell passaging. Western blots of cell lysates of passaged *Akt*-null lung fibroblasts engineered to express *Akt1*, *Akt2*, or *Akt3* were probed with *Akt* isoform-specific antibodies. Tubulin was used as the loading control. (B) Growth curves of the same cells show that the *Akt3*-expressing cells grow more slowly, while *Akt2*-expressing cells grow at an intermediate rate. *Akt1/2/3*: *Akt* null cells engineered to express all three isoforms.

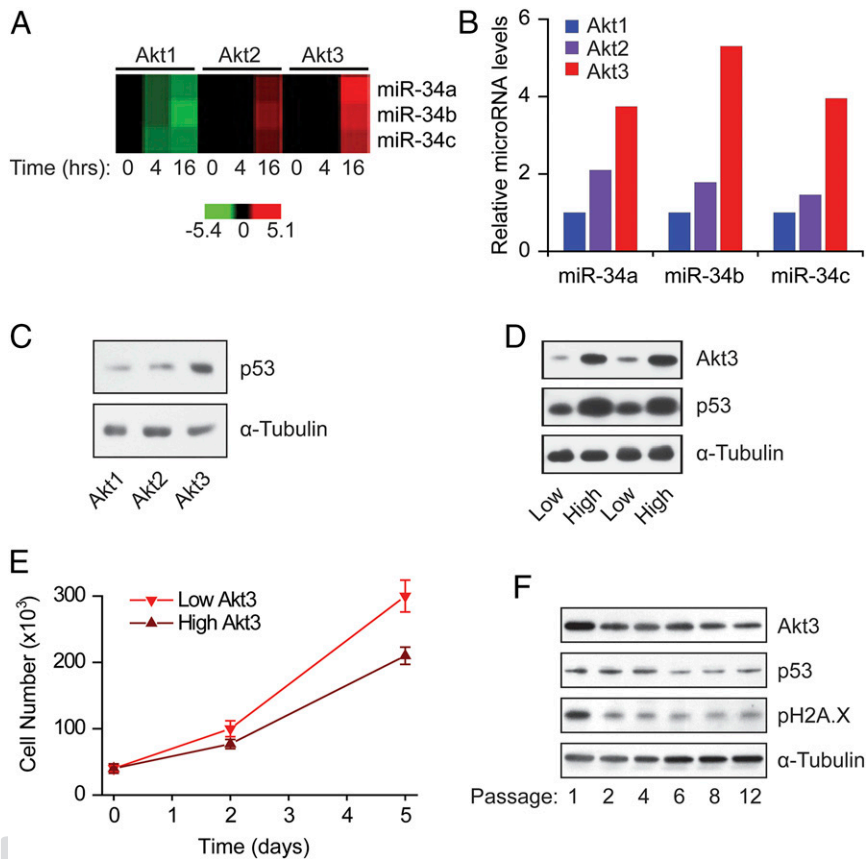


Fig. 2. Akt3 expression activates the DNA damage response. (A) Heatmap showing that treatment with IGF1 induces miR-34a, miR-34b, and miR-34c in Akt3-expressing, and to a lesser extent, in Akt2-expressing cells. (B) Quantitative RT-PCR comparing the expression of miR-34a, miR-34b, and miR-34c in Akt1-, Akt2-, and Akt3-expressing cells growing in serum-containing media. (C) Western blot showing the expression of p53 in cell lysates of Akt1-, Akt2-, and Akt3-expressing cells growing in serum-supplemented media. Tubulin was used as the loading control. (D) Western blot showing the expression of p53 in independent cultures of lung fibroblasts expressing high and low levels of Akt3 (two independent cultures of each). Tubulin was used as the loading control. (E) Growth curves of cells expressing high and low levels of Akt3. (F) Serial passage of Akt3-expressing cells selects for cells expressing progressively lower levels of Akt3. Western blots show that Akt3 expression correlates with the expression of p53 and with the level of H2A.X phosphorylation on Ser139. Tubulin was used as the loading control.

However, in cells growing in serum-supplemented media, the GSH/GSSG ratio was the lowest in cells expressing Akt3 (*SI Appendix, Fig. S5*), as expected. In agreement with these data, the abundance of oxidized proteins, detected by probing immunoblots of whole cell extracts with an antibody that recognizes carbonyl groups in cellular proteins, was also the highest in the Akt3-, followed by the Akt1-rescued cells (Fig. 3F).

The Activation of the DNA Damage Response in Akt3-Rescued Cells Is ROS Dependent. The preceding data (Figs. 1–3) suggested that the slow growth of Akt3-expressing cells is due to the accumulation of ROS, which induces DNA damage and consequently activates the p53 response pathway. To address this hypothesis, we examined the effects of the ROS scavenger NAC on the proliferation of Akt1-, Akt2-, and Akt3-expressing cells. The results revealed that NAC stimulates cellular proliferation in the Akt3-rescued, but not in the Akt1- and Akt2-rescued cells (Fig. 4A, B, and C). Moreover, NAC suppresses the expression of p53 (Fig. 4D) and miR-34 (Fig. 4E) in Akt3-expressing cells. These data support the proposed hypothesis.

The Akt3-Mediated Suppression of Cellular Proliferation via ROS Is p53 and INK4a/Arf Dependent. To determine whether the induction of p53 by ROS in Akt3-expressing cells is required for the Akt3-mediated inhibition of cellular proliferation, wild-type MEFs and *p53*^{-/-} MEFs were transduced with retroviral constructs of

Akt1 or Akt3. Western blot analysis verified that Akt3 overexpression induces the expression of p53 (*SI Appendix, Fig. S6*), while cell growth assays revealed that Akt3 overexpression inhibits the proliferation of wild-type MEFs (Fig. 5A), but does not affect the proliferation of *p53*^{-/-} cells (Fig. 5B). Measurements of DHE- and DCFDA-detectable ROS (superoxide and H₂O₂, respectively) by flow cytometry confirmed that both are selectively induced by Akt3 in both wild-type and *p53*^{-/-} cells (Fig. 5C and D). Based on these data we conclude that the inhibition of cellular proliferation by Akt3-induced ROS is indeed p53 dependent. To investigate the involvement of p53 in miR-34 regulation downstream of Akt3, we examined the effects of Akt3 overexpression on the levels of miR-34 family members in wild-type and *p53*^{-/-} MEFs. qRT-PCR analysis revealed that the induction of miR-34a, b and c, depends at least in part on p53 (*SI Appendix, Fig. S7*). To assess the role of miR-34 in Akt3-mediated suppression of cell proliferation, we inhibited miR-34 activity by antisense oligos. Inhibition of miR-34 increased the rate of proliferation of Akt3-rescued cells by 15% with no effects on Akt1-expressing cells (*SI Appendix, Fig. S8*), suggesting that miR-34 plays a minor role, relative to other p53-dependent mechanisms.

In addition to p53, DNA damage activates the *INK4a/Arf* locus, which encodes the p16^{INK4a}, p15^{INK4b}, and p19^{Arf} proteins (p14^{Arf} in humans) (54, 55). The cyclin-dependent kinase inhibitors p16^{INK4a} and p15^{INK4b} regulate the phosphorylation of the retinoblastoma (Rb) family members, in cells traversing the

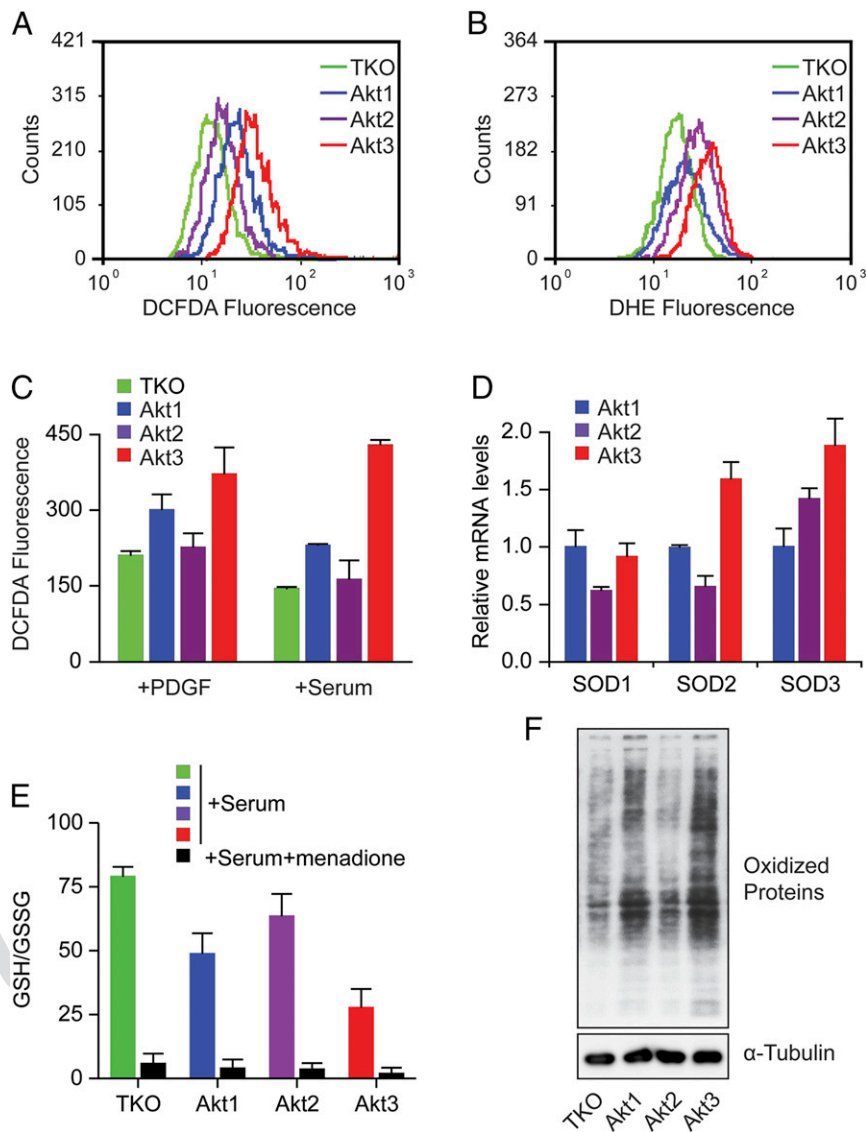


Fig. 3. ROS are differentially regulated by the three Akt isoforms. (A) Flow cytometry of TKO, Akt1-, Akt2-, and Akt3-expressing cells growing in serum-supplemented media and treated with DCFDA. (B) Flow cytometry of TKO, Akt1-, Akt2-, and Akt3-expressing cells growing in complete serum-supplemented media and treated with DHE. (C) DCFDA-detectable fluorescence in TKO, Akt1-, Akt2-, and Akt3-expressing cells, 10 min after treatment with PDGF or serum. (D) Expression of SOD1, SOD2, and SOD3 was determined by qRT-PCR in Akt1-, Akt2-, and Akt3-expressing cells growing in complete serum-supplemented media. (E) Ratio of reduced-to-oxidized glutathione (GSH/GSSG) in TKO, Akt1-, Akt2-, and Akt3-expressing cells growing in complete serum-supplemented media was determined by spectrophotometric (412 nm) measurement of 5,5'-dithiobis(2-nitrobenzoic acid) (DTNB) reduction to 2-nitro-5-thiobenzoic acid (TNB) in deproteinized cell lysates and are expressed in nanomoles per milliliter (nmol/mL). Cells pretreated with oxidative menadione (40 μ M) to increase GSSG, were used as positive controls. (F) Western blot of cell lysates from TKO, Akt1-, Akt2-, and Akt3-expressing lung fibroblasts, probed with an antibody recognizing carbonyl groups on protein side chains. Such groups reflect the oxidation status of proteins. Tubulin was used as the loading control. TKO: Akt-null (triple knockout) cells.

G1 phase of the cell cycle, while p19^{Arf} regulates the abundance of p53. Based on these considerations, we examined whether the Akt3-mediated inhibition of cell proliferation depends also on the INK4/ARF locus. To this end, MEFs in which both INK4 and ARF were ablated (*INK4a*^{-/-}/*Arf*^{-/-}), and MEFs in which ARF was selectively ablated (*Arf*^{-/-}), were transduced with retroviral constructs of Akt1 or Akt3. The results confirmed that the expression of Akt3 does not suppress the proliferation of these cells (Fig. 5 E and F). We conclude that the inhibition of cellular proliferation by Akt3 depends not only on p53, but also on the *INK4a/ARF* locus. Collectively, our data indicate that the ROS-mediated inhibition of cellular proliferation in Akt3-expressing cells depends on the activation of the DNA damage response.

Akt3 Inhibits Cell Proliferation by Promoting ROS Production via Phosphorylation of p47^{phox} and Activation of the NADPH Oxidase. The levels of ROS in cells expressing different Akt isoforms may be due to the differential regulation of ROS production or ROS detoxification by Akt1, Akt2, and Akt3 (*SI Appendix, Fig. S1*). To address this question, we employed an assay that measures the overall antioxidant activity in cell lysates. The results (*SI Appendix, Fig. S9*) revealed that Akt3-expressing cells exhibit high, rather than low antioxidant activity, suggesting that Akt3 may up-regulate ROS by promoting ROS production rather than by inhibiting ROS detoxification and that feedback mechanisms up-regulate antioxidant activity to detoxify the increased levels of ROS.

Akt3 may stimulate ROS production by one of two mechanisms: 1) It may stimulate mitochondrial biogenesis and mitochondrial

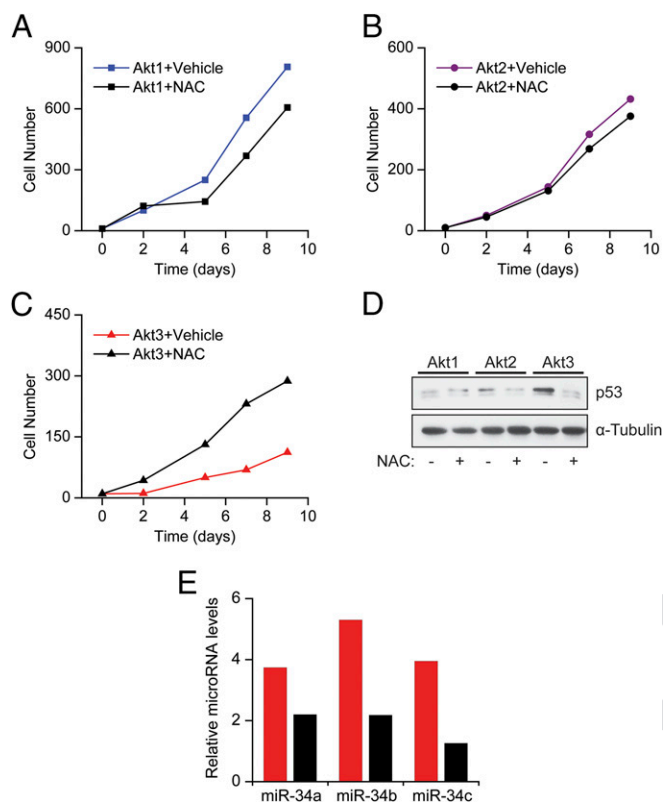


Fig. 4. The slow proliferation of Akt3-expressing cells is ROS dependent. (A–C) Growth curves of Akt1-, Akt2-, and Akt3-expressing cells before and after treatment with the antioxidant NAC. The antioxidant was renewed every 3 d. (D) Western blot showing the expression of p53 in Akt1-, Akt2-, and Akt3-expressing cells before and after treatment with NAC. Tubulin was used as the loading control. (E) Quantitative RT-PCR comparing the expression of miR-34a, miR-34b, and miR-34c in Akt3-expressing cells before and after treatment with NAC.

oxidative phosphorylation. This mechanism appears to play an important role in Akt3-mediated ROS production in VEGF-stimulated endothelial cells (56). 2) It may activate the NADPH oxidase by phosphorylating components of the enzyme complex. Phosphorylation of p47^{phox}, one of the regulatory components of the NADPH oxidase, at Ser304 and Ser328, had indeed been observed in earlier studies addressing the effects of Akt on the activity of purified NADPH oxidase in vitro (51, 57, 58). Experiments using the ROS-activated fluorescent dye mitotracker, which monitors ROS levels in the mitochondria, revealed that all Akt isoforms up-regulate mitochondrial ROS with similar efficiencies (SI Appendix, Fig. S10). Moreover, parallel experiments revealed that the induction of DCFDA-detectable ROS (H₂O₂), which is more robust in Akt3-expressing cells, is completely blocked by the NADPH oxidase inhibitors 4-(2-aminoethyl)benzenesulfonyl fluoride hydrochloride (AEBSF) and diphenyleneiodonium (DPI) (SI Appendix, Figs. S11 and S12). These observations combined suggested that ROS are produced in response to growth factor signals that are transduced by Akt (primarily Akt3), and activate the NADPH oxidase. To test this hypothesis, we expressed the Flag-tagged p47^{phox} in lung fibroblasts expressing one Akt isoform at a time. Cell lysates were immunoprecipitated by anti-Flag (p47^{phox}), and Western blots were probed with the phosphorylated Akt substrate (RXXS*/I*) antibody. This approach demonstrated that Akt3 phosphorylates p47^{phox} more efficiently than Akt1 or Akt2 (Fig. 6A). Importantly, in Akt3-expressing cells, p47^{phox} phosphorylation was lost by treatment with the Akt inhibitor MK2206 (SI Appendix, Fig. S13).

To link p47^{phox} phosphorylation and NADPH activity, spontaneously immortalized p47^{phox}-/- MEFs were transduced with Akt1 or Akt3 retroviral constructs. Transduced cells were subsequently compared to determine whether they differ in p53 expression, cell proliferation rates, and in DCFDA- and DHE-detectable ROS levels. The results showed that both the rates of proliferation (Fig. 6B) and p53 protein levels (Fig. 6C) were similar in Akt1- and Akt3-expressing p47^{phox}-/- MEFs, and accordingly, the ability of Akt3 to induce miR-34 was impaired (SI Appendix, Fig. S14). Importantly, the differences between Akt1- and Akt3-induced ROS observed in wild-type MEFs (Fig. 5C) were diminished in p47^{phox}-/- MEFs (Fig. 6D and E). We conclude that Akt3 induces ROS and subsequently p53 expression by activating the NADPH oxidase.

To determine whether NADPH oxidase is preferentially regulated by Akt3, we transduced p47^{phox}-/- MEFs with wild-type p47^{phox} and retroviral constructs of Akt1 or Akt3. Control p47^{phox}-rescued p47^{phox}-/- cells were transduced with the empty retroviral vector (pBabe puro). DHE (superoxide) fluorescence monitored by flow cytometry was significantly more robust in cells transduced with Akt3 than in cells transduced with Akt1 or with the empty vector (Fig. 6F). To determine whether Akt3 enhances ROS production by phosphorylating p47^{phox}, we mutated both phosphorylation motifs of p47^{phox} (Fig. 6G). Spontaneously immortalized MEFs from p47^{phox}-/- mice were transduced with retroviral constructs of Flag-tagged wild-type p47^{phox} or the Flag-tagged phosphorylation site mutants [p47^{phox}S304A, p47^{phox}S328A, or p47^{phox}S304A/S328A (DMp47phox)]. The same cells were superinfected with retroviral constructs of Akt1 or Akt3. Transduced cells were analyzed for p47^{phox} phosphorylation by probing anti-Flag immunoprecipitates with the Akt phosphosubstrate antibody. The same cells were treated with DHE and they were analyzed by flow cytometry. The results confirmed that the Ser304 and Ser328 sites were both phosphorylated by Akt (primarily Akt3) in vivo. Notably, although the phosphorylation of the single mutants is higher in the Akt3 than in the Akt1-expressing cells, the background phosphorylation of the double mutant by Akt1 and Akt3 is equal (Fig. 6H). They also confirmed that, whereas Akt3 significantly up-regulates superoxide in p47^{phox}-/- MEFs rescued with the wild-type p47^{phox}, neither Akt3 nor Akt1 up-regulates superoxide in MEFs rescued with the phosphorylation site mutant of p47^{phox} (Fig. 6I). We conclude that ROS induction by Akt3 depends on the NADPH oxidase which is preferentially activated by Akt3 via phosphorylation of p47^{phox} at Ser304 and Ser328.

Akt3 Regulates the Expression of p53, and Cancer Cells Adapt to the Akt3-p53 Axis. The link between Akt3 and p53 was also observed in human cancer cell lines. Comparison of the p53 levels in three melanoma cell lines, of which one (SKMEL2) expresses high levels of Akt3 and two (LoxMVII and UACC62) express low levels of Akt3, revealed that the levels of Akt3 correlate with the levels of p53 (SI Appendix, Fig. S15A). More important, knockdown of Akt3 in SKMEL2 cells suppressed p53 levels (SI Appendix, Fig. S15B), suggesting that p53 expression is under the control of Akt3. The above observation was validated in breast cancer cell lines expressing all Akt isoforms (T-47D, MDA-MB-231). Whereas, silencing of Akt3 in both cell lines resulted in suppression of p53, knockdown of Akt1 or Akt2 had minimal effects (Fig. 7A and B).

Akt3 is highly expressed in several tumor types (68–70). Interrogation of cancer genomics datasets (TCGA: The Cancer Genome Atlas) through the cBioportal website (71, 72), revealed that the *Akt3* gene is genetically altered, most commonly amplified, in numerous types of human cancer (SI Appendix, Fig. S16). Given the antiproliferative effects of Akt3, the selection of tumor cells with an amplified and/or overexpressed *Akt3* gene is a paradox. To address this paradox, we hypothesized that cells adapt to the overexpression of Akt3 by inactivating the DNA damage response pathway. To address this hypothesis, we employed data

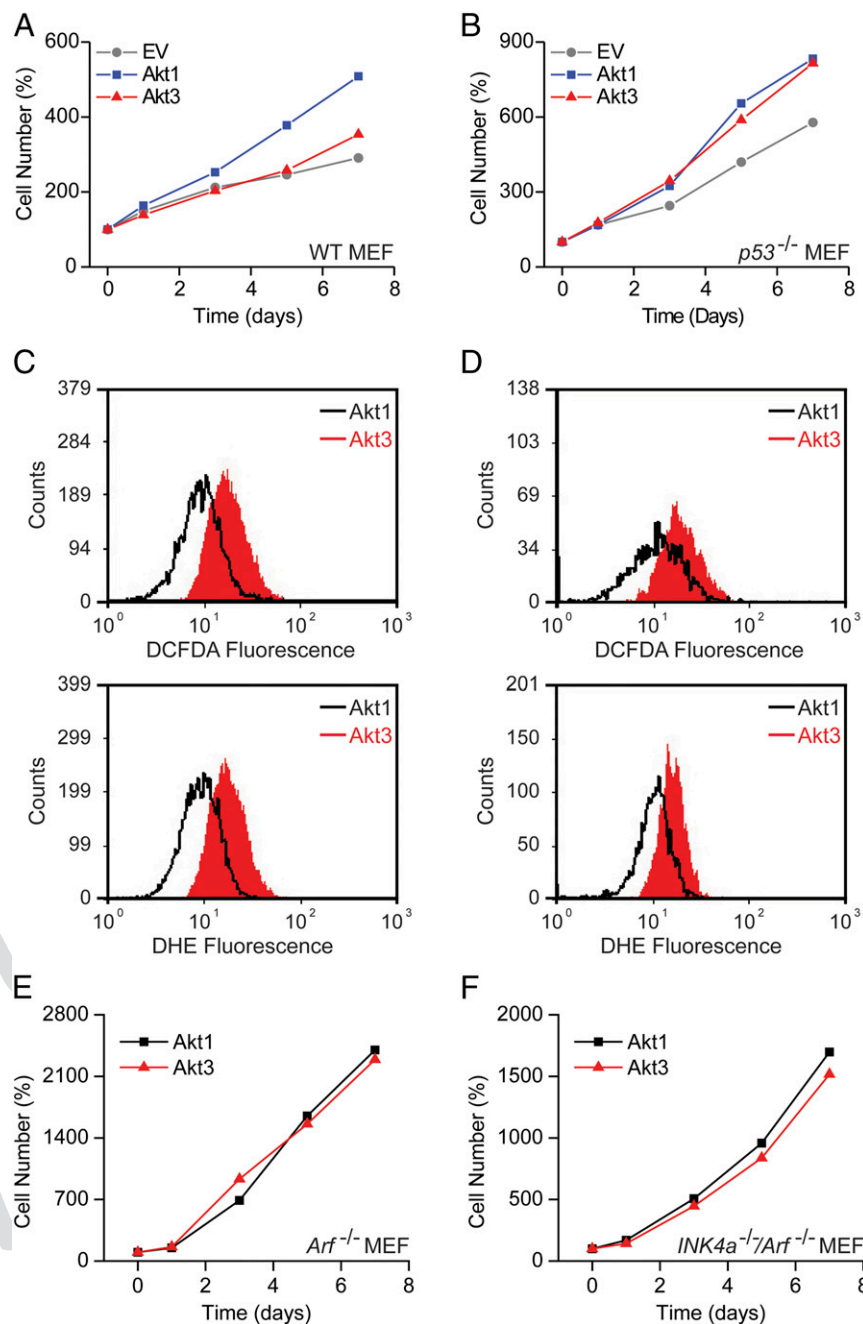


Fig. 5. The growth inhibitory effects of Akt3 are p53 and INK4A/ARF dependent. (A and B) Growth curves of wild-type (A) and $p53^{-/-}$ (B) MEFs transfected with Akt1, Akt3, or the empty vector, and growing in complete serum-supplemented media. (C and D) DCFDA- and DHE-detectable ROS were measured by flow cytometry in the Akt1- and Akt3-expressing wild-type (C) and $p53^{-/-}$ (D) MEFs. (E and F) Growth curves of $Arf^{-/-}$ (E) or $INK4a^{-/-}/Arf^{-/-}$ (F) MEFs, expressing Akt1 or Akt3 and growing in serum-supplemented media.

extracted from the OncoPrint database to examine the correlation between Akt3 and p53 expression. These analyses revealed that in three types of human cancer [melanomas (Fig. 7C), breast (Fig. 7D), and lung carcinomas (Fig. 7E)], the expression of Akt3 exhibits an excellent positive correlation with the expression of p53. Moreover, the frequency of p53 mutation is significantly higher in tumors with Akt3 amplification than in tumors without Akt3 alterations (Fig. 7F).

Discussion

Data presented in this report address the role of individual Akt isoforms in the generation of ROS. The initial experiments were

carried out in immortalized lung fibroblasts, which were engineered to express one Akt isoform at a time, but were otherwise identical (30–33). A screen comparing these cells with each other and with isogenic Akt-null cells for the abundance of ROS showed that although all Akt isoforms contribute to ROS generation, it is Akt3 that is the most robust ROS inducer. These studies were initiated because of the observation that Akt3-expressing cells grow significantly slower than Akt1- or Akt2-expressing isogenic cells and their slow growth is associated with high levels of p53 and high levels of the microRNAs miR-34a, miR-34b, and miR-34c, which are direct transcriptional targets of p53. The elevation of p53 was due to the activation of

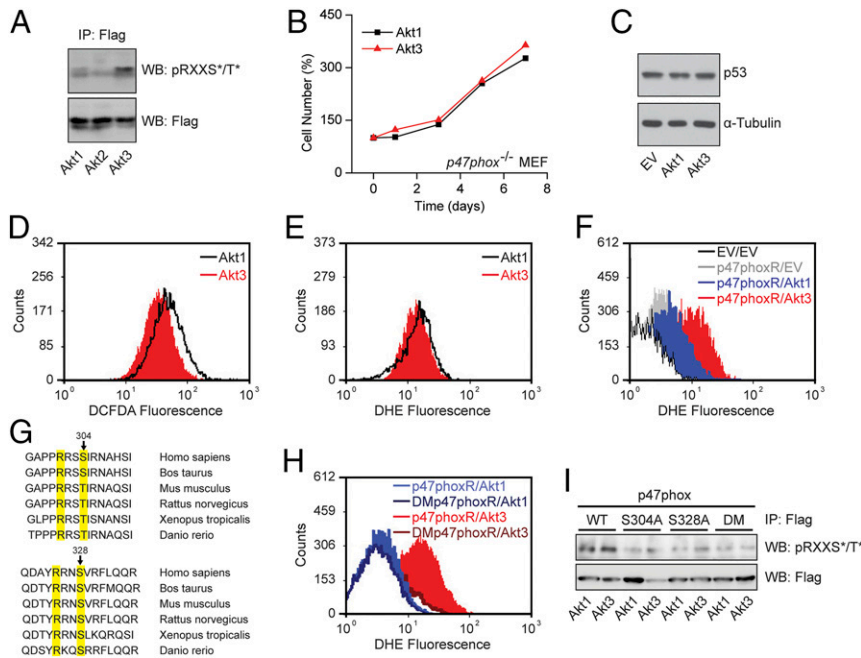


Fig. 6. The slow proliferation of Akt3-expressing cells is caused by ROS, induced by Akt3, via $p47^{\text{phox}}$ phosphorylation, and activation of the NADPH oxidase. (A) Phosphorylation of $p47^{\text{phox}}$ in Akt1-, Akt2-, and Akt3-expressing cells growing in serum-supplemented media. Akt1-, Akt2-, and Akt3-expressing lung fibroblasts were transduced with wild-type Flag- $p47^{\text{phox}}$. $p47^{\text{phox}}$ was immunoprecipitated from cell lysates with an anti-Flag antibody. A Western blot of the immunoprecipitates was probed with an Akt phosphosubstrate antibody (RXXS*/T*). The same immunoprecipitates were probed with the anti-Flag antibody (loading control). (B) Growth curves of $p47^{\text{phox-/-}}$ MEFs expressing Akt1 or Akt3 and growing in complete serum-supplemented media. (C) Western blot showing the expression of p53 in cell lysates of Akt1- and Akt3-expressing $p47^{\text{phox-/-}}$ MEFs growing in serum-supplemented media. Tubulin was used as the loading control. (D and E) DCFDA- and DHE-detectable ROS in the Akt1- and Akt3-expressing $p47^{\text{phox-/-}}$ MEFs were measured by flow cytometry. (F) DHE-detectable ROS levels were measured by flow cytometry, in $p47^{\text{phox-/-}}$ MEFs and their derivatives, transduced with the empty vector (pBabe-neo) or with wild-type $p47^{\text{phox}}$ ($p47^{\text{phoxR}}$). The wild-type $p47^{\text{phox-}}$ -rescued cells were also transduced with Akt1 or Akt3 retroviral constructs or with the empty vector (EV). (G) Conservation of the Akt phosphorylation motifs, RXXS*/T, on $p47^{\text{phox}}$ (Ser304 and Ser328). (H) Phosphorylation of wild type and $p47^{\text{phox}}$ mutants in Akt1- and Akt3-expressing cells growing in serum-supplemented media. Akt1- and Akt3-expressing lung fibroblasts were transduced with wild-type Flag- $p47^{\text{phox}}$ (WT) or its mutants Flag- $p47^{\text{phoxS304A}}$, Flag- $p47^{\text{phoxS328A}}$, or Flag- $p47^{\text{phoxS304A/S328A}}$ double mutant (DM). Cell lysates were immunoprecipitated with the anti-Flag antibody ($p47^{\text{phox}}$), and Western blots of the immunoprecipitates were probed with the Akt phosphosubstrate antibody (RXXS*/T*). Probing immunoprecipitates with anti-Flag antibody was used as the loading control. The same immunoprecipitates probed with anti-Flag were used as the loading control. (I) DHE-detectable ROS, measured by flow cytometry, in $p47^{\text{phox-/-}}$ MEFs and their derivatives, transduced with the wild-type $p47^{\text{phox}}$ ($p47^{\text{phoxR}}$) or the double phosphorylation site mutant of $p47^{\text{phox}}$ (DM $p47^{\text{phoxR}}$). Both the wild type and the mutant $p47^{\text{phox-}}$ -rescued cells were also transduced with Akt1 or Akt3 retroviral constructs. EV/EV, cells transduced with both empty vectors; R, rescued.

the DNA damage response by reactive oxygen species, whose levels were significantly higher in the Akt3-expressing cells. The importance of ROS in the activation of the DNA damage response in the Akt3-expressing cells was confirmed both by pharmacologic and genetic experiments. Specifically, we showed that the antioxidant NAC reduced the levels of p53 and promoted cell proliferation selectively in Akt3-expressing cells. Moreover, Akt3 expression failed to inhibit cell proliferation when expressed in $p53^{-/-}$, $INK4a^{-/-}/Arf^{-/-}$, and $Arf^{-/-}$ cells, despite the fact that the loss of these genes had no effect on the up-regulation of ROS by Akt3. Further studies revealed that the robust up-regulation of ROS by Akt3, as opposed to Akt1 and Akt2, is due to differences between Akt isoforms in the generation rather than the clearance of ROS.

The induction of ROS by Akt has been described previously (48–51). However, most of the earlier studies do not distinguish between Akt isoforms and they focus primarily on the role of Akt in the regulation of ROS detoxification mechanisms. Thus, it has been observed that Akt phosphorylates and inactivates the FOXO family of transcription factors, which normally promote the expression of the mitochondrial enzyme MnSOD (SOD2) (73, 74). ROS induction by Akt and other oncogenes also promotes the expression of FOXM1, another member of the forkhead family of transcription factors, which induces the expression of several ROS detoxifying enzymes, including MnSOD, catalase, and PRDX3 (75). Importantly, Akt also stabilizes NRF2 and promotes the

expression of regulators of glutathione synthesis, resulting in glutathione up-regulation (76). These Akt-regulated activities may be important for the overall regulation of ROS by Akt; however, they do not seem to contribute to the differential induction of ROS by Akt3. First, Akt3 is a more robust inducer of ROS than the other Akt isoforms, and it functions by stimulating ROS generation rather than by inhibiting ROS detoxification. Second, the expression of SOD2 and SOD3 is higher in Akt3-expressing, relative to the Akt1- and Akt2-expressing cells, while the expression of SOD1 is equivalent in Akt3- and Akt1-expressing cells. Significantly, SOD1 and SOD2 expression is higher in Akt1- than in Akt2-expressing cells and this correlates with the levels of H_2O_2 and superoxide in the two cell types, with the levels of H_2O_2 (DCFDA-detectable ROS) being higher in Akt1-expressing cells and the levels of superoxide (DHE-detectable ROS) being higher in Akt2-expressing cells. We have not addressed the mechanism of this difference. However, we have observed that Akt2-expressing cells tend to express higher levels of p53 and microRNAs of the miR-34 family and they proliferate slower than the Akt1-expressing cells.

In the experiments presented here, the high levels of ROS in the Akt3-expressing cells were induced by growth factor stimulation, and they were not associated with the mitochondria. More detailed analyses showed that the Akt3-dependent stimulation of ROS production was due to the phosphorylation of the NADPH oxidase subunit $p47^{\text{phox}}$, which results in NADPH activation. Previous studies had shown that NADPH oxidase can be activated

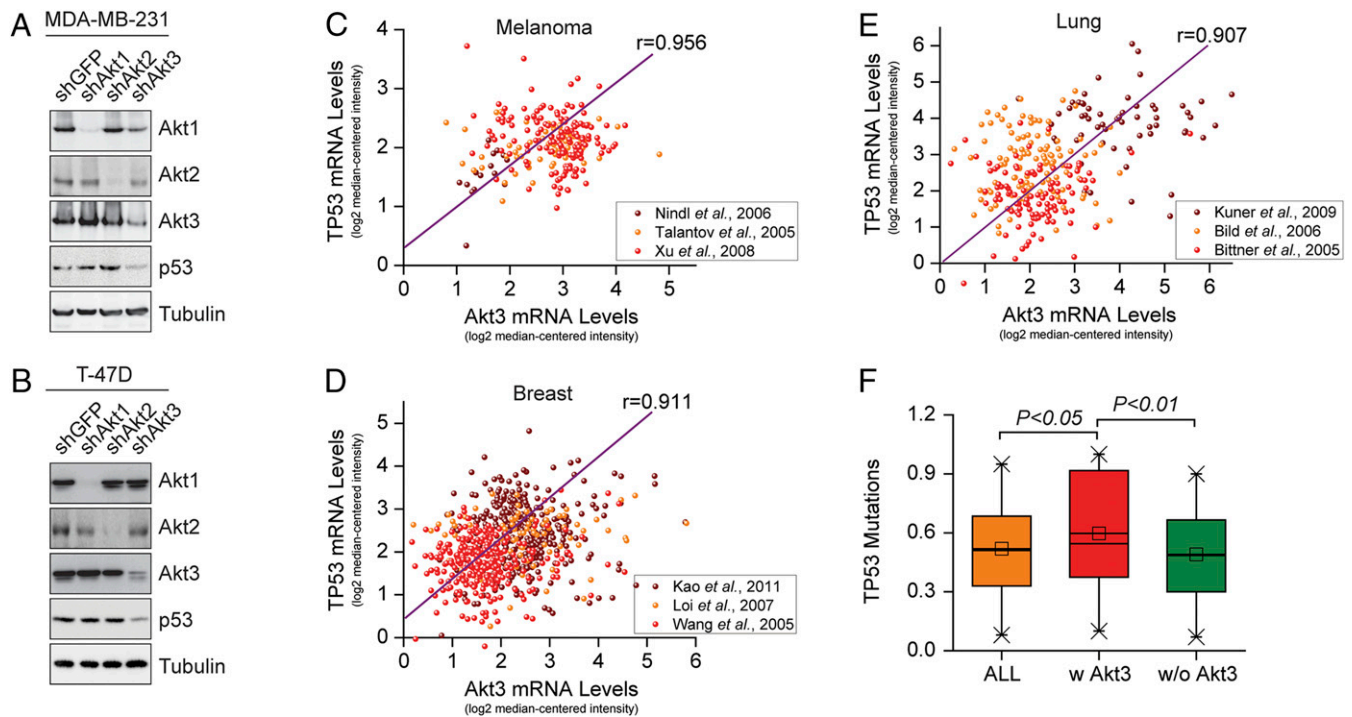


Fig. 7. The expression of Akt3 in multiple human tumor types correlates with the expression of p53. Mechanisms of tumor cell adaptation to Akt3 expression. (A and B) Akt1, Akt2, or Akt3 were knocked down in the high Akt3-expressing breast cancer cell lines MDA-MB-231 (A) and T-47D (B). Western blots of lysates derived from these and control cells (shGFP) were probed with antibodies against Akt1, Akt2, Akt3, p53, and tubulin (loading control). (C–E) Analysis of data obtained from Oncomine, shows that the abundance of p53 mRNA (probe ID number 201746_at) correlates with the abundance of Akt3 mRNA (probe ID number 212607_at) in human melanomas (59–61) (C), breast (62–64) (D), and lung (65–67) (E) carcinomas. (F) Akt3 amplification or mutation in human tumors correlates with the deletion or mutation of p53. Analysis of data was obtained from the cBioportal for Cancer Genomics. Data compiled from 36 different studies with Akt3 alterations ranging from 0.3 to 34% were plotted to show the frequency of p53 genetic alterations in tumors with or without alterations in Akt3 (statistical comparisons with the paired sample t test).

via the Akt-mediated phosphorylation of p47^{phox} at two conserved sites (51, 57) (Fig. 6). However, these data were obtained from biochemical in vitro experiments, which were carried out using purified proteins. In addition, they did not distinguish between Akt isoforms. The experiments presented here provide in vivo confirmation of the in vitro biochemical data. In addition, they address the roles of the three Akt isoforms and they explore the biological consequences of p47^{phox} phosphorylation in live cells. An earlier study focusing on the role of Akt3 in ROS induction in endothelial cells had shown that Akt3 promotes the generation of ROS by stimulating mitochondrial biogenesis (56). The data presented in this report did not directly address the role of Akt3 in mitochondrial biogenesis. However, the earlier study failed to show a disproportionate increase in mitochondrial ROS following Akt3 activation. It is possible that the difference between this and the earlier study showing the effects of Akt3 on mitochondrial biogenesis is in the types of cells used in these studies.

The high expression of p53 in Akt3-expressing cells suppresses cell proliferation. The overexpression of Akt3 in human melanomas and other types of human tumors therefore is puzzling, because it would be expected to inhibit the proliferation of the tumor cells. We therefore hypothesized that these tumors may have undergone genetic or epigenetic changes that allow them to tolerate the high Akt3 levels. These changes may result in the deregulation of the DNA damage response pathways. Data extracted from the Oncomine and TCGA databases support this conclusion by showing that in several types of cancer, Akt3 levels positively

correlate with the levels of p53 and that p53 mutations are more common in tumors with a genetically altered (most commonly amplified) Akt3, than in tumors with a normal Akt3 gene. Cells with impaired DNA damage response and high levels of ROS would be expected to exhibit significant genetic instability, which may contribute to the aggressiveness of these tumors. Akt3 activity may result in loss of the p53 “brake” but due to high levels of ROS and/or DNA damage maintain high ATM and Rad3-related serine/threonine kinase (ATR)/checkpoint kinase 1 (CHK1) activity (77, 78). Based on the promising data from ongoing clinical trials with ATR/CHK1 inhibitors (79), we propose that these inhibitors could prove effective against tumors with high Akt3 activity.

In summary, although all Akt isoforms promote the up-regulation of ROS, Akt3 is the Akt isoform most efficiently up-regulating ROS. ROS up-regulation by Akt3 is due primarily to the phosphorylation of p47^{phox}, which activates the NADPH oxidase. ROS induction induces the DNA damage response and inhibits cell proliferation. Therefore, tumor cells expressing high levels of Akt3 adapt to grow by inactivating the DNA damage response, which allows them to bypass the inhibitory effects of ROS on cell proliferation.

Data Availability. All study data are included in the article and supporting information.

ACKNOWLEDGMENTS. This work was supported by NIH grant R01 CA186729 to P.N.T. and NTU quality research (QR) funds to C.P. and M.H.

1. R. Radi, Oxygen radicals, nitric oxide, and peroxynitrite: Redox pathways in molecular medicine. *Proc. Natl. Acad. Sci. U.S.A.* **115**, 5839–5848 (2018).
2. D. P. Jones, Radical-free biology of oxidative stress. *Am. J. Physiol. Cell Physiol.* **295**, C849–C868 (2008).

3. S. S. Sabharwal, P. T. Schumacker, Mitochondrial ROS in cancer: Initiators, amplifiers or an achilles' heel? *Nat. Rev. Cancer* **14**, 709–721 (2014).
4. J. Yan, J. Jiang, L. He, L. Chen, Mitochondrial superoxide/hydrogen peroxide: An emerging therapeutic target for metabolic diseases. *Free Radic. Biol. Med.* **152**, 33–42 (2020).

5. A. Panday, M. K. Sahoo, D. Osorio, S. Batra, NADPH oxidases: An overview from structure to innate immunity-associated pathologies. *Cell. Mol. Immunol.* **12**, 5–23 (2015).
6. J. El-Benna *et al.*, Priming of the neutrophil respiratory burst: Role in host defense and inflammation. *Immunol. Rev.* **273**, 180–193 (2016).
7. A. M. Franchini, D. Hunt, J. A. Melendez, J. R. Drake, FcγR-driven release of IL-6 by macrophages requires NOX2-dependent production of reactive oxygen species. *J. Biol. Chem.* **288**, 25098–25108 (2013).
8. H. Buvelot, V. Jaquet, K. H. Krause, Mammalian NADPH oxidases. *Methods Mol. Biol.* **1982**, 17–36 (2019).
9. I. S. Mudway, F. J. Kelly, S. T. Holgate, Oxidative stress in air pollution research. *Free Radic. Biol. Med.* **151**, 2–6 (2020).
10. R. P. Brandes, N. Weissmann, K. Schröder, Nox family NADPH oxidases: Molecular mechanisms of activation. *Free Radic. Biol. Med.* **76**, 208–226 (2014).
11. Y. Zhang, P. Murguesan, K. Huang, H. Cai, NADPH oxidases and oxidase crosstalk in cardiovascular diseases: Novel therapeutic targets. *Nat. Rev. Cardiol.* **17**, 170–194 (2020).
12. M. Takahashi *et al.*, Protein kinase A-dependent phosphorylation of Rap1 regulates its membrane localization and cell migration. *J. Biol. Chem.* **288**, 27712–27723 (2013).
13. S. J. Forrester, D. S. Kikuchi, M. S. Hernandez, Q. Xu, K. K. Griendling, Reactive oxygen species in metabolic and inflammatory signaling. *Circ. Res.* **122**, 877–902 (2018).
14. D. A. Mogilenko *et al.*, Metabolic and innate immune cues merge into a specific inflammatory response via the UPR. *Cell* **177**, 1201–1216.e19 (2019).
15. G. Martel-Gallegos *et al.*, Oxidative stress induced by P2X7 receptor stimulation in murine macrophages is mediated by c-Src/Pyk2 and ERK1/2. *Biochim. Biophys. Acta* **1830**, 4650–4659 (2013).
16. N. T. Moldogazieva, S. V. Lutsenko, A. A. Terentiev, Reactive oxygen and nitrogen species-induced protein modifications: Implication in carcinogenesis and anticancer therapy. *Cancer Res.* **78**, 6040–6047 (2018).
17. H. Sies, D. P. Jones, Reactive oxygen species (ROS) as pleiotropic physiological signalling agents. *Nat. Rev. Mol. Cell Biol.* **21**, 363–383 (2020).
18. N. Krishnan *et al.*, Harnessing insulin- and leptin-induced oxidation of PTP1B for therapeutic development. *Nat. Commun.* **9**, 283 (2018).
19. Y. Heun *et al.*, Inactivation of the tyrosine phosphatase SHP-2 drives vascular dysfunction in Sepsis. *EBioMedicine* **42**, 120–132 (2019).
20. J. Kwon *et al.*, Reversible oxidation and inactivation of the tumor suppressor PTEN in cells stimulated with peptide growth factors. *Proc. Natl. Acad. Sci. U.S.A.* **101**, 16419–16424 (2004).
21. H. Kong, N. S. Chandel, Regulation of redox balance in cancer and T cells. *J. Biol. Chem.* **293**, 7499–7507 (2018).
22. C. Polyarchou, M. Hatziaepostolou, E. Papatimitriou, Hydrogen peroxide stimulates proliferation and migration of human prostate cancer cells through activation of activator protein-1 and up-regulation of the heparin affini regulatory peptide gene. *J. Biol. Chem.* **280**, 40428–40435 (2005).
23. C. Y. Han *et al.*, NADPH oxidase-derived reactive oxygen species increases expression of monocyte chemotactic factor genes in cultured adipocytes. *J. Biol. Chem.* **287**, 10379–10393 (2012).
24. V. I. Lushchak, Free radicals, reactive oxygen species, oxidative stress and its classification. *Chem. Biol. Interact.* **224**, 164–175 (2014).
25. B. Morgan *et al.*, Multiple glutathione disulfide removal pathways mediate cytosolic redox homeostasis. *Nat. Chem. Biol.* **9**, 119–125 (2013).
26. T. F. Franke *et al.*, The protein kinase encoded by the Akt proto-oncogene is a target of the PDGF-activated phosphatidylinositol 3-kinase. *Cell* **81**, 727–736 (1995).
27. B. D. Manning, L. C. Cantley, AKT/PKB signaling: Navigating downstream. *Cell* **129**, 1261–1274 (2007).
28. A. Bellacosa, J. R. Testa, S. P. Staal, P. N. Tsichlis, A retroviral oncogene, akt, encoding a serine-threonine kinase containing an SH2-like region. *Science* **254**, 274–277 (1991).
29. L. C. Cantley, B. G. Neel, New insights into tumor suppression: PTEN suppresses tumor formation by restraining the phosphoinositide 3-kinase/AKT pathway. *Proc. Natl. Acad. Sci. U.S.A.* **96**, 4240–4245 (1999).
30. I. Sanidas *et al.*, Phosphoproteomics screen reveals akt isoform-specific signals linking RNA processing to lung cancer. *Mol. Cell* **53**, 577–590 (2014).
31. S. A. Ezell *et al.*, The protein kinase Akt1 regulates the interferon response through phosphorylation of the transcriptional repressor EMSY. *Proc. Natl. Acad. Sci. U.S.A.* **109**, E613–E621 (2012).
32. C. Polyarchou *et al.*, Akt2 regulates all Akt isoforms and promotes resistance to hypoxia through induction of miR-21 upon oxygen deprivation. *Cancer Res.* **71**, 4720–4731 (2011).
33. D. Iliopoulos *et al.*, MicroRNAs differentially regulated by Akt isoforms control EMT and stem cell renewal in cancer cells. *Sci. Signal.* **2**, ra62 (2009).
34. W. S. Chen *et al.*, Growth retardation and increased apoptosis in mice with homozygous disruption of the Akt1 gene. *Genes Dev.* **15**, 2203–2208 (2001).
35. H. Cho, J. L. Thorvaldsen, Q. Chu, F. Feng, M. J. Birnbaum, Akt1/PKBalpha is required for normal growth but dispensable for maintenance of glucose homeostasis in mice. *J. Biol. Chem.* **276**, 38349–38352 (2001).
36. S. H. Jackson, J. I. Gallin, S. M. Holland, The p47phox mouse knock-out model of chronic granulomatous disease. *J. Exp. Med.* **182**, 751–758 (1995).
37. L. A. Donehower *et al.*, Mice deficient for p53 are developmentally normal but susceptible to spontaneous tumours. *Nature* **356**, 215–221 (1992).
38. M. Serrano *et al.*, Role of the INK4a locus in tumor suppression and cell mortality. *Cell* **85**, 27–37 (1996).
39. C. Polyarchou, R. Pfau, M. Hatziaepostolou, P. N. Tsichlis, The JmjC domain histone demethylase Ndy1 regulates redox homeostasis and protects cells from oxidative stress. *Mol. Cell Biol.* **28**, 7451–7464 (2008).
40. L. He *et al.*, A microRNA component of the p53 tumour suppressor network. *Nature* **447**, 1130–1134 (2007).
41. A. J. Levine, W. Hu, Z. Feng, The P53 pathway: What questions remain to be explored? *Cell Death Differ.* **13**, 1027–1036 (2006).
42. L. J. Ko, C. Prives, p53: Puzzle and paradigm. *Genes Dev.* **10**, 1054–1072 (1996).
43. D. P. Lane, Cancer, p53, guardian of the genome. *Nature* **358**, 15–16 (1992).
44. K. H. Vousden, D. P. Lane, p53 in health and disease. *Nat. Rev. Mol. Cell Biol.* **8**, 275–283 (2007).
45. J. Yuan, R. Adamski, J. Chen, Focus on histone variant H2AX: To be or not to be. *FEBS Lett.* **584**, 3717–3724 (2010).
46. S. Burma, B. P. Chen, M. Murphy, A. Kurimasa, D. J. Chen, ATM phosphorylates histone H2AX in response to DNA double-strand breaks. *J. Biol. Chem.* **276**, 42462–42467 (2001).
47. A. V. Budanov, The role of tumor suppressor p53 in the antioxidant defense and metabolism. *Subcell. Biochem.* **85**, 337–358 (2014).
48. P. V. Usatyuk *et al.*, Role of c-Met/phosphatidylinositol 3-kinase (PI3k)/Akt signaling in hepatocyte growth factor (HGF)-mediated lamellipodia formation, reactive oxygen species (ROS) generation, and motility of lung endothelial cells. *J. Biol. Chem.* **289**, 13476–13491 (2014).
49. S. Chatterjee *et al.*, Membrane depolarization is the trigger for PI3K/Akt activation and leads to the generation of ROS. *Am. J. Physiol. Heart Circ. Physiol.* **302**, H105–H114 (2012).
50. B. Govindarajan *et al.*, Overexpression of Akt converts radial growth melanoma to vertical growth melanoma. *J. Clin. Invest.* **117**, 719–729 (2007).
51. Q. Chen *et al.*, Akt phosphorylates p47phox and mediates respiratory burst activity in human neutrophils. *J. Immunol.* **170**, 5302–5308 (2003).
52. P. Wardman, Fluorescent and luminescent probes for measurement of oxidative and nitrosative species in cells and tissues: Progress, pitfalls, and prospects. *Free Radic. Biol. Med.* **43**, 995–1022 (2007).
53. I. N. Zelko, T. J. Mariani, R. J. Folz, Superoxide dismutase multigene family: A comparison of the CuZn-SOD (SOD1), Mn-SOD (SOD2), and EC-SOD (SOD3) gene structures, evolution, and expression. *Free Radic. Biol. Med.* **33**, 337–349 (2002).
54. T. Sperka, J. Wang, K. L. Rudolph, DNA damage checkpoints in stem cells, ageing and cancer. *Nat. Rev. Mol. Cell Biol.* **13**, 579–590 (2012).
55. W. Y. Kim, N. E. Sharpless, The regulation of INK4/ARF in cancer and aging. *Cell* **127**, 265–275 (2006).
56. Y. Wang *et al.*, Regulation of VEGF-induced endothelial cell migration by mitochondrial reactive oxygen species. *Am. J. Physiol. Cell Physiol.* **301**, C695–C704 (2011).
57. C. R. Hoyal *et al.*, Modulation of p47PHOX activity by site-specific phosphorylation: Akt-dependent activation of the NADPH oxidase. *Proc. Natl. Acad. Sci. U.S.A.* **100**, 5130–5135 (2003).
58. J. Chen, H. Tang, N. Hay, J. Xu, R. D. Ye, Akt isoforms differentially regulate neutrophil functions. *Blood* **115**, 4237–4246 (2010).
59. L. Xu *et al.*, Gene expression changes in an animal melanoma model correlate with aggressiveness of human melanoma metastases. *Mol. Cancer Res.* **6**, 760–769 (2008).
60. D. Talantov *et al.*, Novel genes associated with malignant melanoma but not benign melanocytic lesions. *Clin. Cancer Res.* **11**, 7234–7242 (2005).
61. I. Nindl *et al.*, Identification of differentially expressed genes in cutaneous squamous cell carcinoma by microarray expression profiling. *Mol. Cancer* **5**, 30 (2006).
62. K. J. Kao, K. M. Chang, H. C. Hsu, A. T. Huang, Correlation of microarray-based breast cancer molecular subtypes and clinical outcomes: implications for treatment optimization. *BMC Cancer* **11**, 143 (2011).
63. S. Loi *et al.*, Definition of clinically distinct molecular subtypes in estrogen receptor-positive breast carcinomas through genomic grade. *J. Clin. Oncol.* **25**, 1239–1246 (2007).
64. Y. Wang *et al.*, Gene-expression profiles to predict distant metastasis of lymph-node-negative primary breast cancer. *Lancet* **365**, 671–679 (2005).
65. R. Kuner *et al.*, Global gene expression analysis reveals specific patterns of cell junctions in non-small cell lung cancer subtypes. *Lung Cancer* **63**, 32–38 (2009).
66. A. H. Bild *et al.*, Oncogenic pathway signatures in human cancers as a guide to targeted therapies. *Nature* **439**, 353–357 (2006).
67. M. Bittner *et al.*, "Expression Project for Oncology (expO)." NCBI Gene Expression Omnibus. <http://www.ncbi.nlm.nih.gov/geo/query/acc.cgi?acc=GSE2109>. Accessed 18 October 2020.
68. Y. R. Chin *et al.*, Targeting Akt3 signaling in triple-negative breast cancer. *Cancer Res.* **74**, 964–973 (2014).
69. S. Banerji *et al.*, Sequence analysis of mutations and translocations across breast cancer subtypes. *Nature* **486**, 405–409 (2012).
70. J. M. Stahl *et al.*, Deregulated Akt3 activity promotes development of malignant melanoma. *Cancer Res.* **64**, 7002–7010 (2004).
71. J. Gao *et al.*, Integrative analysis of complex cancer genomics and clinical profiles using the cBioPortal. *Sci. Signal.* **6**, p11 (2013).
72. E. Cerami *et al.*, The cBio cancer genomics portal: An open platform for exploring multidimensional cancer genomics data. *Cancer Discov.* **2**, 401–404 (2012).
73. J. Guo, Z. Gertsberg, N. Ozgen, S. F. Steinberg, p66Shc links alpha1-adrenergic receptors to a reactive oxygen species-dependent AKT-FOXO3A phosphorylation pathway in cardiomyocytes. *Circ. Res.* **104**, 660–669 (2009).
74. D. R. Calnan, A. Brunet, The FoxO code. *Oncogene* **27**, 2276–2288 (2008).
75. H. J. Park *et al.*, FoxM1, a critical regulator of oxidative stress during oncogenesis. *EMBO J.* **28**, 2908–2918 (2009).
76. E. C. Lien *et al.*, Glutathione biosynthesis is a metabolic vulnerability in PI(3)K/Akt-driven breast cancer. *Nat. Cell Biol.* **18**, 572–578 (2016).
77. T. Katsube *et al.*, Most hydrogen peroxide-induced histone H2AX phosphorylation is mediated by ATR and is not dependent on DNA double-strand breaks. *J. Biochem.* **156**, 85–95 (2014).
78. J. Willis, Y. Patel, B. L. Lentz, S. Yan, APE2 is required for ATR-Chk1 checkpoint activation in response to oxidative stress. *Proc. Natl. Acad. Sci. U.S.A.* **110**, 10592–10597 (2013).
79. E. Lecona, O. Fernandez-Capetillo, Targeting ATR in cancer. *Nat. Rev. Cancer* **18**, 586–595 (2018).